Effects of Surge Tank Geometry on the Water Hammer Phenomenon: Numerical Investigation

Mohammad Mahmoudi-Rad (m.m6456@yahoo.com)
Higher Educational Complex of Bam
Mohammad Najafzadeh
Graduate University of Advanced Technology

Research Article

Keywords: Water hammer, Transient flow fluctuations, Method of characteristics, Surge Tank

Posted Date: June 3rd, 2021

DOI: https://doi.org/10.21203/rs.3.rs-572430/v1

Effects of Surge Tank Geometry on the Water Hammer Phenomenon: Numerical Investigation

Mohammad Mahmoudi-Rad[1*] and Mohammad Najafzadeh[2]

[1]Assistant Professor, Department of Civil Engineering, Higher Education Complex of Bam, P.O. Box 76615314, Bam, Iran (corresponding author). E-mail: m.m6456@yahoo.com; m.mahmoudirad@bam.ac.ir

[2] Associate Professor, Department of Water Engineering, Faculty of Civil and Surveying Engineering, Graduate University of Advanced Technology, P.O. Box 76315116, Kerman, Iran. E-mail: moha.najafzadeh@gmail.com; m.najafzadeh@kgut.ac.ir

Abstract

A surge tank, as one of the most common control facilities, is applied to control head pressure level in long pressurized pipelines during the water hammer occurrence. The cost-effective operation of surge tank is highly affected by its characteristics (i.e., surge tank diameter and inlet diameter of surge tank) and can effectively reduce the repercussion of water hammer. This investigation utilized the method of characteristics (MOC) in order to simulate the behavior of transient flow at surge tank upstream and head pressure fluctuations regime for hydraulic system of a hydropower dam. The various types of boundary conditions (i.e., sure tank, reservoir, branch connection of three pipes, series pipes, and downstream valve) were applied to numerically investigate the simultaneous effects of the surge tank properties. In this way, all the simulations of water hammer equations were conducted for nine various combinations of surge tank diameter (D) and inlet diameter of surge tank (d). Results of this study indicated that, for the surge tank design with D=6m and d=3.4m, head pressure fluctuations reached

minimum level in the large section of pipeline here is surge tank upstream. Additionally, occurrence of water hammer phenomenon was probable at the initial section of pipeline.

Keywords: Water hammer; Transient flow fluctuations; Method of characteristics; Surge Tank

Introduction

Water hammer occurrence is one of the most destructive hydraulic phenomena in the water distribution systems. This issue takes place in the event that flow velocity and pressure values vary suddenly in the some cases such as suddenly opening and closing valves, accidents of pump, and unexpectedly-depressurized hydraulic systems. Overall, water hammer takes place in various hydraulic systems such as pump stations (Wan and Huang, 2011; Hur et al., 2017; Kim et al., 2014; Rohani and Afshar, 2010), hydro-power systems (Guo et. al., 2017; Liu et al., 2017; Riasi and Tazraei, 2017), water-transferring systems (Duan et al., 2010; Kim, 2010; Collins et al., 2012; Zhang et al., 2018; Bettaieb and Taieb, 2020), and oil-transferring systems (Behbahani-Nejad and Bagheri, 2010; Esmaeilzadeh et al., 2009).

Water hammer causes damages in different ways (*i*) severe fluctuations in pressure and noise, (*ii*) cavitation occurrence in the hydraulic systems. Specifically, instant positive and negative pressure occurred during water hammer phenomenon stands at the higher level than operation pressure. Positive pressure causes the damages to the valves and pipe burst whereas negative pressure crushes the pipe systems.

Applying preventative methods to eradicate the repercussions of the water hammer phenomena has become the cornerstone of experts in the hydraulic fields. Through this

issue, the maximum reduction of maximum pressure values and maximum increase of minimum pressure values have drawn significant attention to the control of water hammer occurrences in the recent decades. In this way, these methods generally include installation of control facilities of water hammer and optimization of facilities performance (Wan and Zhang, 2018; Wan et al., 2019). Improvement of policy for the closing valve and coordinated performance of the hydraulic systems is one of the most common optimization methods to control water hammer phenomenon (Bazargan-Lari et al., 2013; Zhou et al., 2017; Wan and Li, 2016).

Moreover, optimizing the performance of the hydraulic systems is not essentially capable of controlling water hammer and there is an occasional need for protective pieces of device for this aim. Generally, surge tanks, relief valves, and pressure tanks are the most well-known pieces of equipment to control the water hammer (Wan et al., 2019). However, surge tanks are one of the most widely used protection devices to reduce the water hammer. These tanks are very popular in water transmission systems, pumping systems and power plant systems. Although large number of attempts were made on surge tanks, they are still being developed to investigate responses of surge tank to the variations of surge tank geometry. It should be noted that severe fluctuations in water level may cause during frequent emptying and filing tank in the water hammer occurrence. Therefore, having a sufficient cross section and vertical height is essential. As a result, the lack of space and necessary height occasionally limit the coordinated operation of surge tanks. However, in the case of the above-mentioned problems, surge tanks are not well capable of controlling the severe fluctuations caused by the water hammer.

74 Laboratory and numerical investigations have been conducted to simulate transient
75 hydraulic flows occurring the water hammer. However, in the case of laboratory
76 simulations, it is very difficult to simultaneously combine various boundary conditions.
77 In addition, performing an experimental study is highly time-consuming time and
78 expensive. With the development of computers and computational methodologies,
79 numerical techniques are being used more widely to simulate the water hammer in
80 various engineering applications. In this case, numerical methods are grouped into three
81 main categories: Finite Difference Method (FDM), Finite Element Method (FEM), and
82 Finite Volume Method (FVM). Over the past few decades, various numerical methods
83 have been developed to simulate and control transient hydraulic flows during the water
84 hammer phenomenon. The most commonly used FDMs is the Method of Characteristics
85 (MOC) with explicit form, which has been widely applied and improved in multi-pipe
86 hydraulic systems (i.e., Karadzic et al., 2014; Holler and Jaberg, 2013; Vasconcelos et al.,
87 2015; Wang and Yang, 2014; Wan and Zhang, 2018).
88 In the recent years, effects of inlet cross-section and length of inlet junction associated
89 with surge tank on the response of surge tank have been investigated (Wang and Yang,
90 2014; Wan et al., 2019). Simultaneous influences of surge tank properties (i.e., surge tank
91 diameter and inlet diameter of surge tank) have not been yet studied. In fact,
92 simultaneous use of surge tank properties causes to find efficient and economic design of
93 water systems. Hence, in this study, the performance of surge tank, installed on the
94 pipeline of Jiroft Dam powerhouse, is studied to reduce the repercussion of water
95 hammer phenomenon. In this way, Method Of Characteristic (MOC), introduced as the
96 most well-known FDMs, is used to simulate the response of water system along with

various boundary conditions in the pipeline such as triple-shaped junction, series pipelines, and control valve at downstream of power plant model.

Overview of Power Plant Model

The power plant case study was constructed for Jiroft Hydroelectric Dam, located at the south east of Iran. The reservoir capacity contains approximately 410 million cubic meters up to 1185*m* above sea level. Fig. 1 shows the details of the hydraulic system of the power plant, including the upstream reservoir, the branch connection of triple pipes, the surge tank, connection of two series pipes, and the valve downstream. The upstream pipe of the surge tank with length 2544 m and diameter 3.4*m* is connected to a three-way junction with the same diameter. The inlet diameter of the surge tank (*d*) and the diameter of the surge tank (*D*) are 3.4*m* and 6*m*, respectively. The system response to the variations in *D* and *d* variables is assessed by ±20% variations in these factors. There are two series pipes with diameters of 2.4*m* and 3.4*m* which placed downstream of power plant model. The friction factor of system pipes is 0.016. In order to investigate and analyze the water hammer phenomenon in different parts of the system, 12 nodes have been located. Nodes 1 to 5 on the upstream pipe, 5 to 7 for the three-way connection, node 8 for the surge tank, nodes 9 and 10 for the series connection of the two pipes, node 11 for the end pipe and node 12 for the control valve at the end of the line path. Pipes are considered. In the initial conditions, the level of the head pressure in nodes 1, 8 and 12 are 67*m*, 62.28*m* and 62.06*m*, respectively.

Equations Governing Transient Flows

The set of physical equations corresponding to fluid motion includes the continuity equation, the motion size equation, and the energy equation. For one-dimensional flow in a closed-ended pipe (as an isothermal process without energy conversion), the governing equations of flow are the equations of continuity and momentum. Therefore, the following equations can be considered for the transient flow regime in the pipe:

$$\begin{cases} L_1 = h_t + \frac{a^2}{g} v_x + v h_x + v \sin\theta = 0 \\ L_2 = v_t + g h_x + v v_x + f \frac{v|v|}{2D_P} = 0 \end{cases} \quad (1)$$

where h is the head pressure, v is the flow velocity, a is the wave speed of water hammer, g is the gravity acceleration, θ is the pipe slope, D_p is the pipeline diameter, t subscript is the derivative of a variable respect to time, and x is derivative of a variable respect to space.

Overview of MOC

The Method Of Characteristics (MOC) has been widely applied to simulate the transient flow for various situations: water pipeline (Zhang et al., 2018; Bettaieb and Taieb, 2020), power plant (Guo et. al., 2017; Liu et al., 2017), and water pump station (; Kim et al., 2014; Hur et al., 2017).

For this purpose, Eq. (1) is converted to the linear combination of L1 and L2 as, $L1+\lambda L2=0$, in which $\lambda=\pm g/a$ and $dx/dt=v\pm a$. In this way, Eq.(1) is re-expressed as,

$$\begin{cases} C^+: \frac{g}{a} h_t + v_t + \frac{g}{a} v \sin\theta + f \frac{v|v|}{2D_P} = 0 \quad , \quad dx/dt = v + a \\ C^-: -\frac{g}{a} h_t + v_t - \frac{g}{a} v \sin\theta + f \frac{v|v|}{2D_P} = 0 \quad , \quad dx/dt = v - a \end{cases} \quad (2)$$

Schematic diagram of MOC was conceptually illustrated in Fig. 2. As seen in Fig. 2, flow velocity and head pressure values which are associated with nodes 2, 3, 4, 11 (see Fig. 1), are obtained as,

$$\begin{cases} C^{+}: (v_P - v_L) + \frac{g}{a}(h_P - h_L) + \frac{g}{a} v_L \sin\theta\,(t_P - t_L) + f\frac{v_L|v_L|}{2D_P}\,(t_P - t_L) = 0 \\ (x_P - x_L) = (v_L + a)(t_P - t_L) \\ C^{-}: (v_P - v_R) - \frac{g}{a}(h_P - h_R) - \frac{g}{a} v_R \sin\theta\,(t_P - t_R) + f\frac{v_R|v_R|}{2D_P}\,(t_P - t_R) = 0 \\ (x_P - x_R) = (v_R - a)(t_P - t_R) \end{cases} \quad (3)$$

In the above-mentioned equation, v_L, v_R, h_L, and h_R are initially computed by interpolation as,

$$\begin{cases} v_L = v_C - a(v_C - v_A)\,\Delta t/\Delta x \\ v_R = v_C - a(v_C - v_B)\,\Delta t/\Delta x \\ h_L = h_C - a(h_C - h_A)\,\Delta t/\Delta x \\ h_R = h_C - a(h_C - h_B)\,\Delta t/\Delta x \end{cases} \quad (4)$$

Eq. (4) is substituted into Eq. (1) and then h_P and v_P are computed as,

$$\begin{cases} v_P = 0.5\left[v_L + v_R + \frac{g}{a}(h_L - h_R) - \frac{g}{a}\Delta t \sin\theta\,(v_L - v_R) - \frac{f\Delta t}{2D_P}(v_L|v_L| + v_R|v_R|)\right] \\ h_P = 0.5\left[h_L + h_R + \frac{a}{g}(v_L - v_R) - \Delta t \sin\theta\,(v_L + v_R) - \frac{a}{g}\frac{f\Delta t}{2D_P}(v_L|v_L| - v_R|v_R|)\right] \end{cases} \quad (5)$$

To compute h_P and v_P for other nodes, boundary conditions need to be investigated.

In this study, the wave speed of transient flow (a) for pipeline at the surge tank upstream (d=3.4m) is 1150 m/s whereas, for pipeline at the surge tank downstream (d=2.4m), is 1300 m/s. To implement MOC for simulation of head pressure and flow velocity variations in the present hydraulic systems, Δt and Δx are fixed as 0.3s and 318m, respectively. Furthermore, MOC programming code was provided in MATLAB.

Boundary conditions

Reservoir upstream

Fig.3 illustrates boundary condition of reservoir upstream. According to this, equation governed by reservoir upstream is expressed as (Chaudhry, 1986),

$$\begin{cases} C^-: & h_{p_{j,1}} = H_{res} \\ & v_{p_{j,1}} = C1_j + C2_j\, h_{p_{j,1}} \\ & C1 = v_R - C2\, h_R + C2\, v_R \sin\theta\ \Delta t - \frac{f\Delta t}{2D_P}\, v_R\, |v_R| \quad , \quad C2 = \frac{a}{g} \end{cases} \tag{6}$$

in which j is the number of pipe and H_{res} is the head pressure of reservoir upstream.

Branch Connection of Three Pipes

According to Fig.1, h_P and v_P are associated with nodes 5, 6, and 7. In fact, boundary condition of branch connection of three pipes was studied by these nodes (5-7). Fig. 4 depicted this typical boundary condition for nodes 5 to 7 and then the following formulation is expressed to find the flow characteristics for these nodes (5 to 7) as (Chaudhry, 1986),

$$\begin{cases} h_{P_{j,n+1}} = \frac{C3_j A_j - C1_{j+1} A_{j+1} - C1_{j+2} A_{j+2}}{C2_j A_j + C2_{j+1} A_{j+1} + C2_{j+2} A_{j+2}} \\ h_{P_{j+1,1}} = h_{P_{j+2,1}} = h_{P_{j,n+1}} \\ v_{p_{j,n+1}} = C3_j - C2_j\, h_{p_{j,n+1}} \\ v_{p_{j+1,1}} = C1_{j+1} + C2_{j+1}\, h_{p_{j+1,1}} \\ v_{p_{j+2,1}} = C1_{j+2} + C2_{j+2}\, h_{p_{j+2,1}} \\ C3 = v_L + C2\, h_L - C2\, v_L \sin\theta\ \Delta t - \frac{f\Delta t}{2D_P}\, v_L\, |v_L| \end{cases} \tag{7}$$

where subscript of n denotes the number of node.

Surge Tank

According to Fig. 5, h_P and v_P values for node 5 are computed as (Chaudhry, 1986),

$$\begin{cases} h_{p_{j+2,n+1}} = L_{j+2} + ZP \\ ZP = z + v_{p_{j+2,n+1}} A_{j+2}\, \Delta t / A_s \\ v_{p_{j+2,n+1}} = (C3_{j+2} - C2_{j+2} h_{p_{j+2,n+1}})/(1 + C2_{j+2} A_{j+2} \Delta t / A_s) \end{cases} \quad (8)$$

Where A_s is the cross-section of surge tank, ZP is the height of water surface in the surge tank at the end of time interval, and z denotes is the height of water surface at the beginning of time interval.

Series Connection

Schematic diagram of series connection boundary condition used in this study was illustrated in Fig.6. The boundary conditions for nodes 9&10 (as seen in Fig. 1) are grouped into typical series connections; therefor, h_p and v_p values are computed as (Chaudhry, 1986),

$$\begin{cases} h_{p_{j,n+1}} = (C3_j A_j - C1_{j+1} A_{j+1})/\left(C2_j A_j + C2_{j+1} A_{j+1}\right) \\ h_{p_{j+1,1}} = h_{p_{j,n+1}} \\ C^+ :\ v_{p_{j,n+1}} = C3_j - C2_j h_{p_{j,n+1}} \\ C^- :\ v_{p_{j+1,1}} = C1_{j+1} + C2_{j+1} h_{p_{j+1,1}} \end{cases} \quad (9)$$

Downstream Valve

Boundary condition of node 12, as illustrated in Fig. 7, includes two states. The first state is the time when valve is closed. This situation is expressed by as $\tau = (1 - t/t_c)$ which t_c is the time duration for valve complete closure.

$$\begin{cases} c_v = {v_0}_j{}^2 / C2_j H_{0_{j,n+1}} \\ C4 = \tau^2 c_v \\ v_{p_{j,n+1}} = \frac{1}{2} C4\left(-1 + \sqrt{1 + 4\frac{C3_j}{C4}}\right. \\ h_{p_{j,n+1}} = (C3_j - v_{p_{j,n+1}})/C2_j \end{cases} \quad (10)$$

where H_0 is the initial head pressure at valve.

The second state of boundary condition is associated with the time when valve is completely closed. In this way, boundary condition for node 12 is expressed as (Chaudhry, 1986),

$$\begin{cases} v_{p_{j,n+1}} = 0 \\ h_{p_{j,n+1}} = C3_j / C2_j \end{cases} \quad (11)$$

Results and Discussion

Response of surge tank

In this section, variation of transient flow characteristics (pressure and velocity) associated whit surge tank are investigated. Fig. 8a illustrates variations of transient head pressure versus time for the surge tank. As seen in Fig. 8a, 9.10 m difference between peak pressure head (H_{max}) and trough pressure head (H_{min}) was depicted in the initially-developed transient flow during fast-closing valve. Difference between H_{max} and H_{min} decreased to 1.08 *m* in the middle of time period. Head pressure of surge tank remained constant (66.56 *m*) in the last of time period. Moreover, variations of transient flow velocity against time (for node 8 in Fig. 1) were illustrated in Fig. 8b. maximum fluctuations of transient flow velocity was 13.76 *m*/*s* at the beginning of transient flow formation and then this value decreased to 1.37 *m*/*s* in the middle time period. Additionally, variations of minimum and maximum head pressure in the surge tank were shown in Fig. 9.

Response of surge tank due to inlet diameter variation

212 Fig. 10 indicates variations of surge tank response versus inlet diameter (*d*). In this study,
213 variations of d were considered as $d \pm 0.2d$. Fig. 10a illustrates variations of head pressure
214 for various surge tank inlet diameters. Maximum variation in the head pressure of surge
215 tank decreased from 9.10 *m* to 8.95 *m* as *d* value increase from 3.4 *m* to 4.08 *m*. In the
216 case of 20% decrease in d value, maximum head pressure remained constant at 9.1 m. As
217 illustrated in Fig. 10a, with passing the time, fluctuations of head pressure for *d*=2.72 *m*
218 stood at the lower level that of *d*=3.4 *m* and 4.08 *m*. Variations of transient flow velocity
219 versus various d values were shown in Fig. 10b. Results indicated that maximum
220 fluctuation of transient flow velocity decreased from 13.76 *m*/*s* in d=3.4 *m* to 9.23 *m*/*s* in
221 d=4.08 *m*. In contrast, as *d* value decreases from 3.4 *m* to 2.72 *m*, maximum fluctuation of
222 flow velocity in the transient state augments from 13.76 *m*/*s* to 20.63 *m*/*s*.
223 With reference to Fig. 11, the pressure head of surge tank was on the rise when flow
224 velocity had positive value. On the contrary, negative values of flow velocity, introduced
225 as flow direction from surge tank to pipeline, cause increase of the head pressure in the
226 surge tank. On the other hand, as the pressure head increased, the surge tank absorbed
227 water from the pipeline to prevent the increase of pressure fluctuation.
228
229 **Response of surge tank due to variations of tank cross sections**
230 In this research, the diameter of surge tank (*D*) varies $\pm 20\% D$ to investigate the response
231 of surge tank. Results showed that variations of the maximum values of head pressure
232 fluctuation in the surge tank versus diameter values has reverse trend in way that values
233 decreased with an increase in *D* values. As illustrated in Fig. 12, the maximum value of
234 head pressure fluctuation increased from 9.10 m in *D*=6 *m* to 9.54 *m* in *D*=4.08 *m*. On the

235 other hand, with an increase of *D* value from 6.0 m to 7.2 m, maximum values of head
236 pressure fluctuation decreased from 9.10 *m* to 8.77 *m*.
237 Furthermore, variations of flow velocity in the transient state versus different values of
238 surge tank diameter were illustrated in Fig. 13. Qualitatively, results indicated that
239 maximum difference of flow velocity values in the node (just under the surge tank) rose
240 from 13.76 *m*/*s* to 16.75 *m*/*s* when *D* values increased from 6.0 *m* to 7.2 *m*. In contract,
241 the maximum difference of flow velocity declined from 13.76 *m*/*s* in *D*=6.0 *m* to 10.66
242 *m*/*s* in *D*=4.08 *m*.
243
244 **Transient flow at upstream of surge tank**
245 Due to existing majority of pipe length between node 1 and node 5, Fig. 14 demonstrated
246 variation of head pressure and flow velocity between nodes 1&5 which placed in the
247 middle and last sections of pipeline. Result demonstrated that maximum value of
248 difference in the head pressure has downward trend, decreasing from 8.62 *m* in node 5 to
249 zero in node 1. In contrast, maximum difference in the flow velocity increased from
250 16.25 *m*/*s* in node 5 to 18.52 *m*/*s* in node 1. The minimum and maximum head pressure
251 values were presented in Fig. 15. According to Fig. 15, the maximum head pressure
252 values were 6.62 *m*, 4.81 *m*, and 3.12 *m* for nodes 4, 3, and 2, respectively.
253
254 **Effects of surge tank inlet diameter on transient flow at upstream of surge tank**
255 As mentioned in the previous section, the maximum difference in the head pressure was
256 on the decline and additionally this trend remained with variations of surge tank inlet
257 diameter. Fig. 16a demonstrated that, for *d*=2.72 *m*, maximum difference in the head

pressure declined from 8.73 *m* in node 5 to zero in node 1. Moreover, for *d*=4.08 *m*, maximum difference in the head pressure decreased from 9.01 *m* in node 5 to zero in node 1 (see Fig. 16b). Therefore, it can be said that variations of surge tank inlet diameter do not prevent the decrease of fluctuation of head pressure at upstream of surge tank.

Table 1 presents flow velocity values for nodes 1 to 5 in the various values of surge tank inlet diameter. As seen in Table 1, maximum difference in the flow velocity at upstream of surge tank has upward trend when inlet diameter of surge tank increased from 2.72 *m* to 4.08 *m*. In fact, fluctuations of flow velocity at upstream of surge tank were affected by decrease of inlet diameter (*d*).

Effects of surge tank diameter on the transient flow at upstream of surge tank

Fig. 17a&b depicted fluctuations of head pressure at upstream of surge tank for different values of *D*. As seen in Fig. 17a&b, maximum difference in pressure head values in the surge tank upstream decreased as diameter of surge tank increased. For *D*=4.8 *m*, maximum difference in the pressure head decreased from 9.17 *m* at node 5 to zero at node 1 (see Fig 17a) and similarity, for *D*=7.2 *m*, maximum value of difference in the pressure head declines from 8.71 *m* at node 5 to zero at node 1 (see Fig 17b).

Fig. 18a&b illustrates fluctuation of flow velocity at upstream of surge tank for various diameter of surge tank. According to Fig. 18a&b the maximum difference in the flow velocity has upward trend at upstream of surge tank as diameter of surge tank increased. For *D*=4.8 *m*, the maximum difference in the flow velocity increased from 14.7 *m*/*s* in node 5 to 16.8 *m*/*s* in node 1 (see Fig 18a). Also, the maximum difference in the flow velocity rose from 17.87 *m*/*s* in node 5 to 19.37 m/s in node 1 for *D*=7.2*m* (see Fig 18b).

Simultaneous effects of surge tank characteristics on the surge tank response

Table 2 presents maximum difference in the pressure head for the three values of surge tank diameter (D) and three values of surge tank inlet diameter (d). In fact, nine combinations for d and D values were provided. As seen in Table 2, for the minimum value of surge tank diameter (d=4.8 m), the fluctuation of head pressure in the surge tank stood at the maximum level when d values had intermediate level (d=3.4 m). Furthermore, values of head pressure fluctuation for both minimum and maximum values of surge tank inlet diameter are approximately the same. Overall, it can be inferred from Table 2 that for all the D values, value of head pressure fluctuation in the surge tank stood at the minimum level for maximum level for maximum level for maximum value of surge tank diameter. In the case of D=6 m, minimum value of head pressure fluctuation obtained 8.95 m for d=4.08 m, for instance. In Table 3, the minimum and maximum values of flow velocity fluctuations at node 8 obtained 7.03 m/s and 24.67 m/s, respectively. In fact, the minimum level of fluctuation (7.03) was associated with d=4.08 m and D=4.8 m while the maximum values of fluctuation was due to d=2.72 m and D=7.2 m. According to the results, when design of surge tank with low diameter and high inlet diameter is desirable, fluctuation of head pressure in the surge tank and fluctuation of flow velocity decreased along with reduction of costs.

Simultaneous effects of surge tank characteristics on the response of upstream

Values of head pressure fluctuations at upstream of surge tank for each combination of d and D were given in Table 4. In minimum value of surge tank diameter (D=4.8 m) for nodes 2 and 5, head pressure fluctuation decreased with increase of d values. On the

304 contrary, this issue had downward trend for nodes 3 and 4. Hence, it can be said that
305 values of head pressure fluctuation in the middle section of upstream pipeline did not
306 stood at the minimum level with lower diameter surge tank and higher value of surge
307 tank inlet diameter. In the nodes 3 to 5, head pressure fluctuations in the middle section
308 of diameter surge tank stood at the higher level for d=2.72 m and 4.08 m than that of
309 d=3.4 m. While, for D=6 m the head pressure fluctuations in the node 2, decreased with
310 an increase of d=3.4 m. Generally, design purpose of surge tank in the middle level of d
311 and D, the head pressure fluctuations in the majority section of upstream surge tank stood
312 at the minimum level for both middle values of surge tank properties (d=3.4 m and D=6
313 m). And more, high risk of water hammer occurrence is probable at the beginning of
314 upstream surge tank. Moreover, for D=7.2 m, head pressure fluctuations decreased at
315 nodes 2 and 4 with an increase of d values while, for node 5, this trend was increasing.
316 Hence, it can be said that design of surge tank with high values of D and d cause to
317 increase probability of water hammer occurrences.
318 Table 5 indicated flow velocity fluctuations in the surge tank upstream for each
319 combination of D and d values. For low value of D, fluctuation of flow velocity stood at
320 the maximum level as d was equal to 3.4 m. Moreover, for D=6 m and 7.2 m, as inlet
321 diameter values of surge tank were 3.4 and 4.08 m, fluctuations of flow velocity were
322 found to be maximum for d=4.08 m. Furthermore, for each value of d, fluctuations of
323 flow velocity at surge tank upstream increased with an increase in diameter of surge tank.
324

325 **Conclusion**

In this research, numerical simulation of water hammer phenomenon was conducted using MOC along with various boundary conditions. Responses of surge tank and upstream pipeline of surge tank to the variations of d and D variables were investigated. In this way, each of d and D variables varied ±20% and therefore, three levels of d (or D) were provided for each geometric factor. Thus, the following conclusions were drawn as,

- Although maximum fluctuation of head pressure in the surge tank for d=2.72m and 3.40m remained constant values, head pressure for d of 2.72m had lower fluctuations than that of d=3.40m.
- Results of MOC simulations indicated that variations of the maximum values of head pressure fluctuations in the surge tank decreased as surge tank diameter got larger.
- At upstream of surge tank (nodes 5 to 1), maximum values of head pressure and maximum values of transient flow velocity had downward and upward trends, respectively.
- The maximum values of fluctuation in the head pressure indicated decreasing trend and then these variations was stable with variations of d values. Fluctuations of flow velocity in the pipeline of surge tank upstream had decreasing trend as d values decreased. Furthermore, upward trend of head pressure fluctuations at the surge tank upstream remained constant with variations of surge tank diameter. For all diameters of surge tank, minimum values of head pressure fluctuations took place for d=4.08m.
- Design of surge tank with low D and high d causes the reduction of construction costs in a way that head pressure fluctuations in the surge tank and flow velocity in the pipeline decreased. In this state, fluctuations of head pressure in the middle sections of pipeline upstream stood at the maximum level and additionally negative consequences of water

hammer need to be prevented. Furthermore, design of surge tank with high values of D and d , risk of water hammer at vicinity of surge tank is higher than other sections of pipeline upstream.

Ethical Approval

All procedures performed in studies involving human participants were in accordance with the ethical standards of the institutional and/or national research committee and with the 1964 Helsinki declaration and its later amendments or comparable ethical standards.

Consent to Participate

Informed consent was obtained from all individual participants included in the study.

Consent to Publish

All the authors give the Publisher the permission of the authors to publish the research work.

Authors Contributions

Mohammad Mahmoudi-rad; Performing the numerical simulation and applying various boundary condition; Analysing results of numerical model; Resources

Mohammad Najafzadeh; Water hammer analysis; Writing - original draft preparation, Writing - review and editing; Supervision

Funding

No funds, grants, or other support was received.

Competing Interests

There is no conflict of interest.

Availability of data and materials

The data are not publicly available due to restrictions such their containing information that

References

Behbahani-Nejad, M., and Bagheri, A. (2010). The accuracy and efficiency of a MATLAB-Simulink library for transient flow simulation of gas pipelines and networks. *Journal of Petroleum Science and Engineering*, *70*(3-4), 256-265.

Bazargan-Lari, M.R., Kerachian, R., Afshar, H., and Bashi-Azghadi, S.N. (2013). Developing an optimal valve closing rule curve for real-time pressure control in pipes. *Journal of Mechanical Science and Technology*, *27*(1), 215-225.

Bettaieb, N. and Taieb, E.H. (2020). Assessment of Failure Modes Caused by Water Hammer and Investigation of Convenient Control Measures. *Journal of Pipeline Systems Engineering and Practice*, *11*(2), 04020006.

Collins, R.P., Boxall, J.B., Karney, B.W., Brunone, B. and Meniconi, S. (2012). How severe can transients be after a sudden depressurization?. *Journal-American Water Works Association*, 104(4), 243-251.

Chaudhry, M.H., (1968). Boundary conditions for analysis of waterhammer in pipe systems. Doctoral dissertation, University of British Columbia.

Duan, H.F., Tung, Y.K. and Ghidaoui, M.S. (2010). Probabilistic analysis of transient design for water supply systems. *Journal of Water Resources Planning and Management*, 136(6), 678-687.

Esmaeilzadeh, F., Mowla, D. and Asemani, M. (2009). Mathematical modeling and simulation of pigging operation in gas and liquid pipelines. *Journal of Petroleum Science and Engineering*, 69(1-2), 100-106.

Guo, W., Yang, J. and Teng, Y. (2017). Surge wave characteristics for hydropower station with upstream series double surge tanks in load rejection transient. *Renewable Energy*, 108, 488-501.

Hoeller, S. and Jaberg, H. (2013). A contribution to water hammer analysis in pumped-storage power plants. *WasserWirtschaft-Hydrologie, Wasserbau, Hydromechanik, Gewässer, Ökologie, Boden*, 103(1/2),78-84.

Hur, J., Kim, S. and Kim, H. (2017). Water hammer analysis that uses the impulse response method for a reservoir-pump pipeline system. *Journal of Mechanical Science and Technology*, 31(10), 4833-4840.

Kim, S.H.(2010). Design of surge tank for water supply systems using the impulse response method with the GA algorithm. *Journal of Mechanical Science and Technology*, *24*(2), 629-636.

Kim, S.G., Lee, K.B. and Kim, K.Y.(2014). Water hammer in the pump-rising pipeline system with an air chamber. *Journal of Hydrodynamics*, 26(6), 960-964.

Karadžić, U., Bulatović, V. and Bergant, A. (2014). Valve-induced water hammer and column separation in a pipeline apparatus. *Strojniški vestnik-Journal of Mechanical Engineering*, 60(11), 742-754.

Liu, J., Zhang, J., Chen, S. and Yu, X. (2017). Investigation on maximum upsurge and air pressure of air cushion surge chamber in hydropower stations. *Journal of Pressure Vessel Technology*, 139(3), 031603.

Rohani, M. and Afshar, M.H. (2010). Simulation of transient flow caused by pump failure: Point-Implicit Method of Characteristics. *Annals of Nuclear Energy*, 37(12), 1742-1750.

Riasi, A. and Tazraei, P. (2017). Numerical analysis of the hydraulic transient response in the presence of surge tanks and relief valves. *Renewable Energy*, *107*, 138-146.

Vasconcelos, J.G., Klaver, P.R. and Lautenbach, D.J. (2015). Flow regime transition simulation incorporating entrapped air pocket effects. *Urban Water Journal*, *12*(6), 488-501.

Wan, W. and Huang, W. (2011). Investigation on complete characteristics and hydraulic transient of centrifugal pump. *Journal of Mechanical Science and Technology*, *25*(10), 2583-2590.

Wang, C. and Yang, J.D. (2015). Water hammer simulation using explicit–implicit coupling methods. *Journal of Hydraulic Engineering*, 141(4), 04014086.

Wan, W. and Li, F. (2016). Sensitivity analysis of operational time differences for a pump–valve system on a water hammer response. *Journal of Pressure Vessel Technology*, 138(1), 011303.

Wan, W., Zhang, B., Chen, X. and Lian, J. (2019). Water hammer control analysis of an intelligent surge tank with spring self-adaptive auxiliary control system. *Energies*, *12*(13), 2527.

Wan, W. and Zhang, B. (2018). Investigation of water hammer protection in water supply pipeline systems using an intelligent self-controlled surge tank. *Energies*, *11*(6), 1450.

Zhou, J., Xu, Y., Zheng, Y. and Zhang, Y. (2017). Optimization of guide vane closing schemes of pumped storage hydro unit using an enhanced multi-objective gravitational search algorithm. *Energies*, *10*(7), 911.

Zhang, B., Wan, W. and Shi, M. (2018). Experimental and numerical simulation of water hammer in gravitational pipe flow with continuous air entrainment. *Water*, *10*(7), 928.

Figures

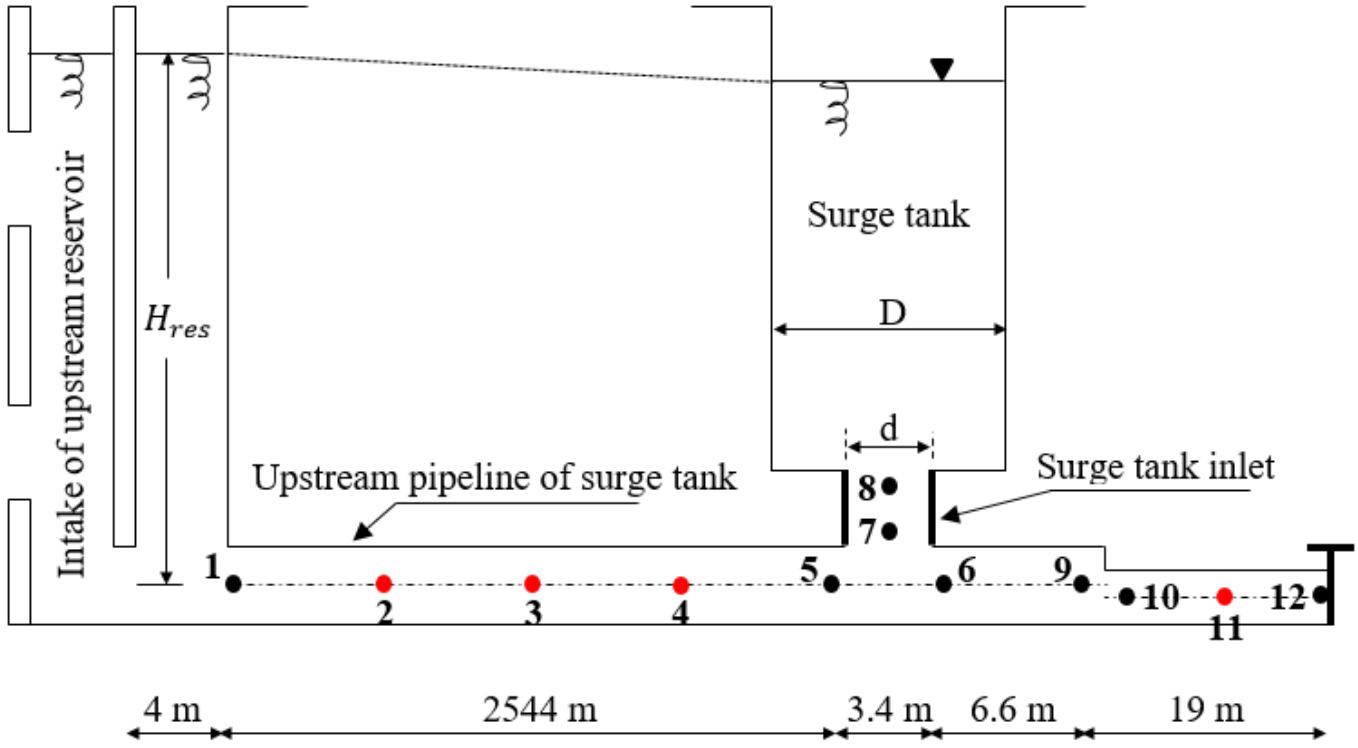

Figure 1

Schematic diagram of the main sections of the power plant

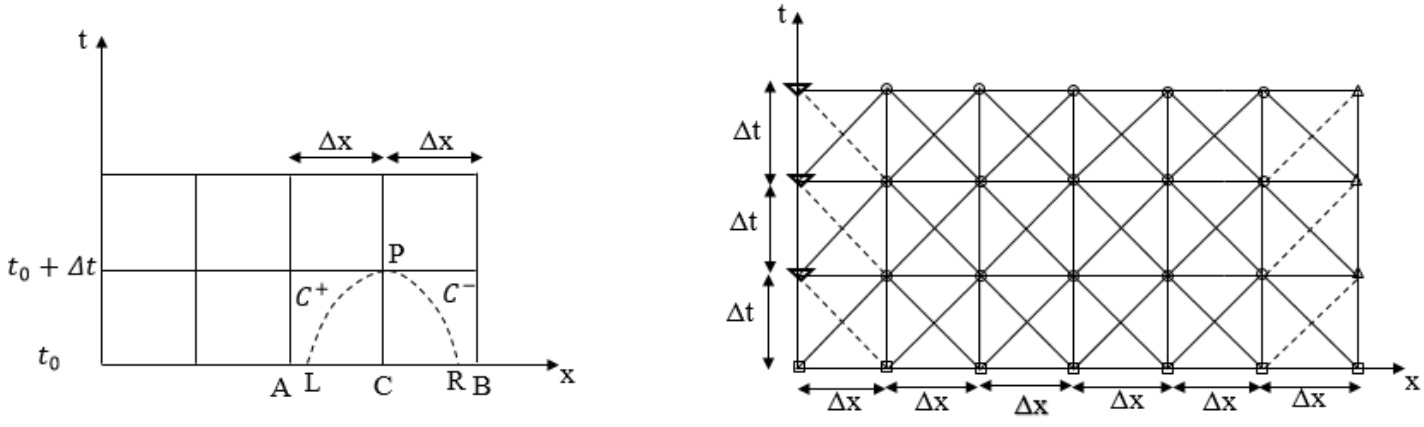

Figure 2

Schematic illustration of MOC

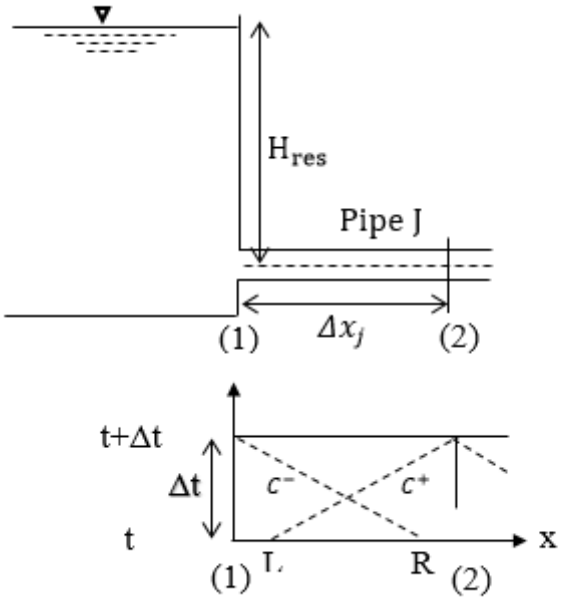

Figure 3

Schematic diagram of boundary condition of reservoir upstream

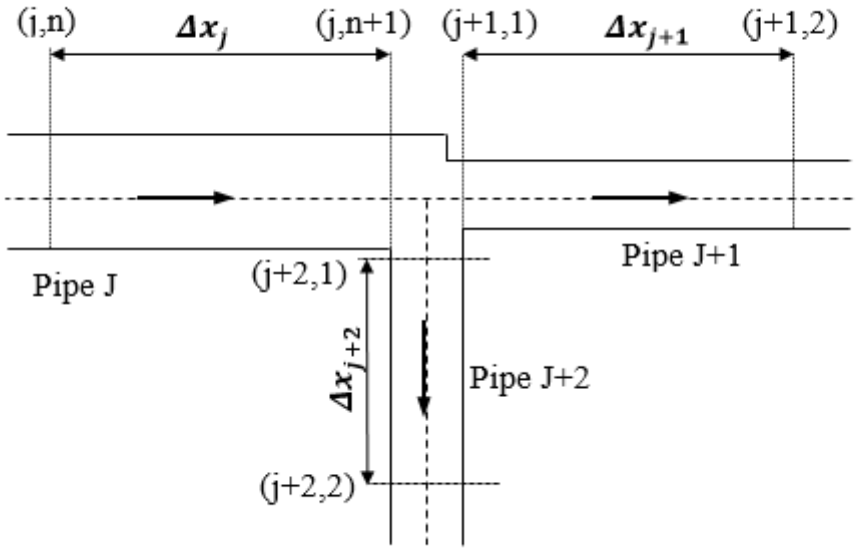

Figure 4

Illustration of boundary condition for branch connection of three pipes

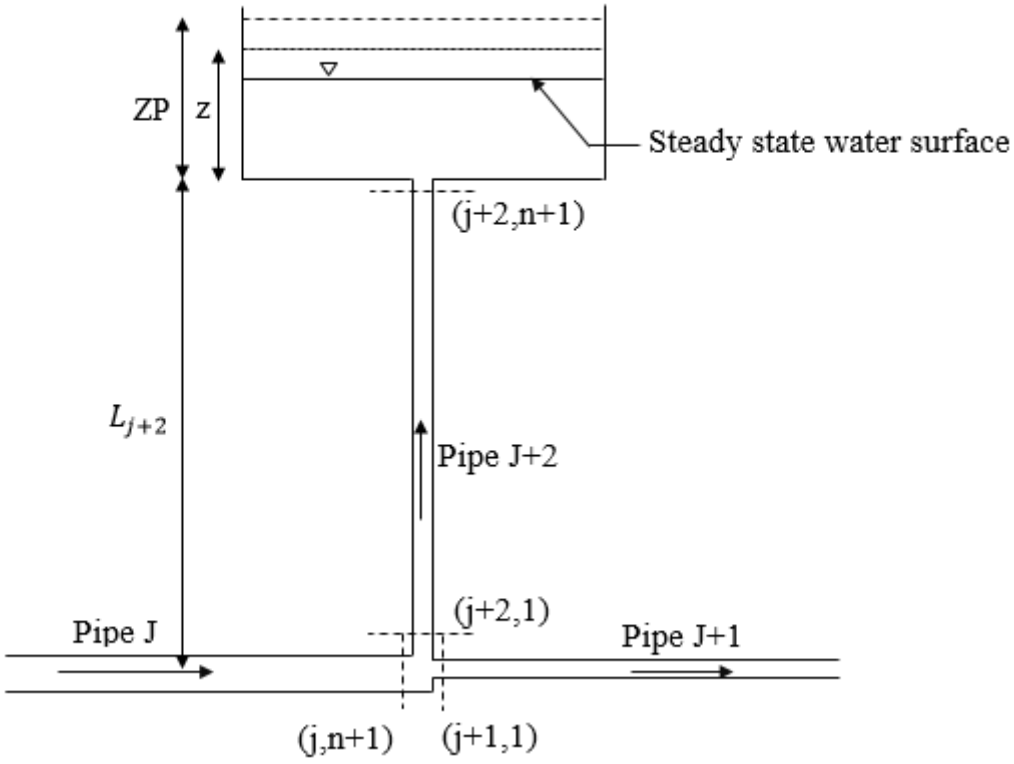

Figure 5

Illustration of boundary condition for surge tank

Figure 6

Conceptual depiction of boundary condition for series connection state

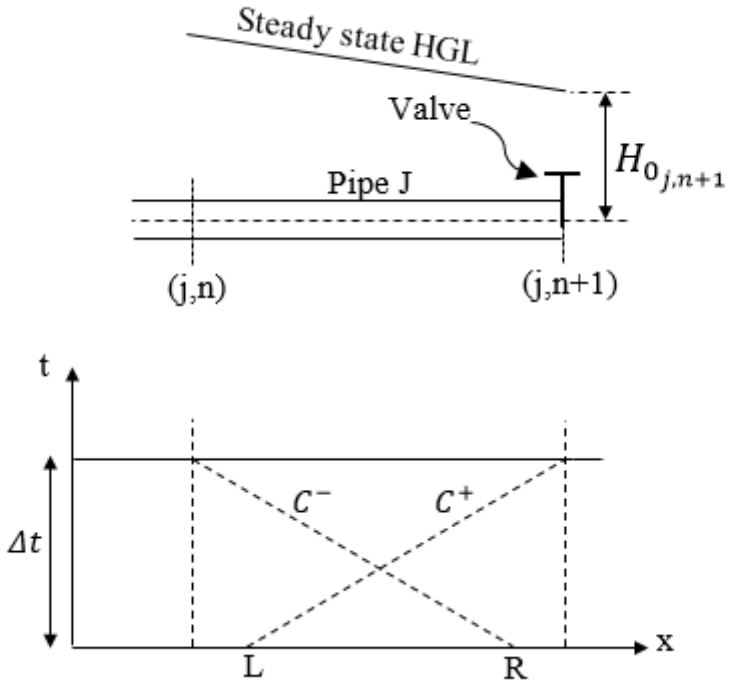

Figure 7

Conceptual depiction of boundary condition for downstream valve state

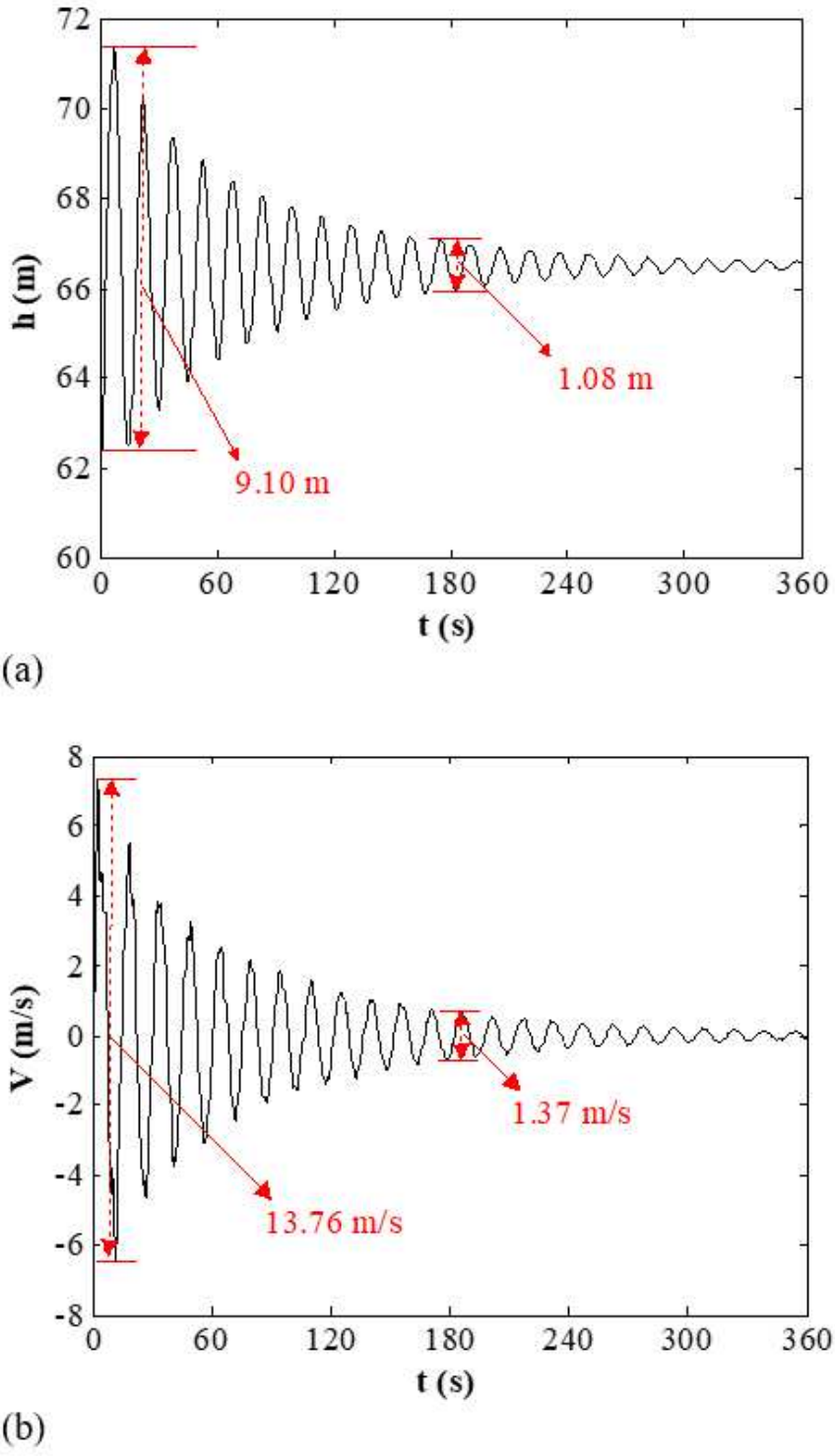

Figure 8

Variations of transient flow properties in the surge tank versus time: (a) head pressure, and (b) flow velocity

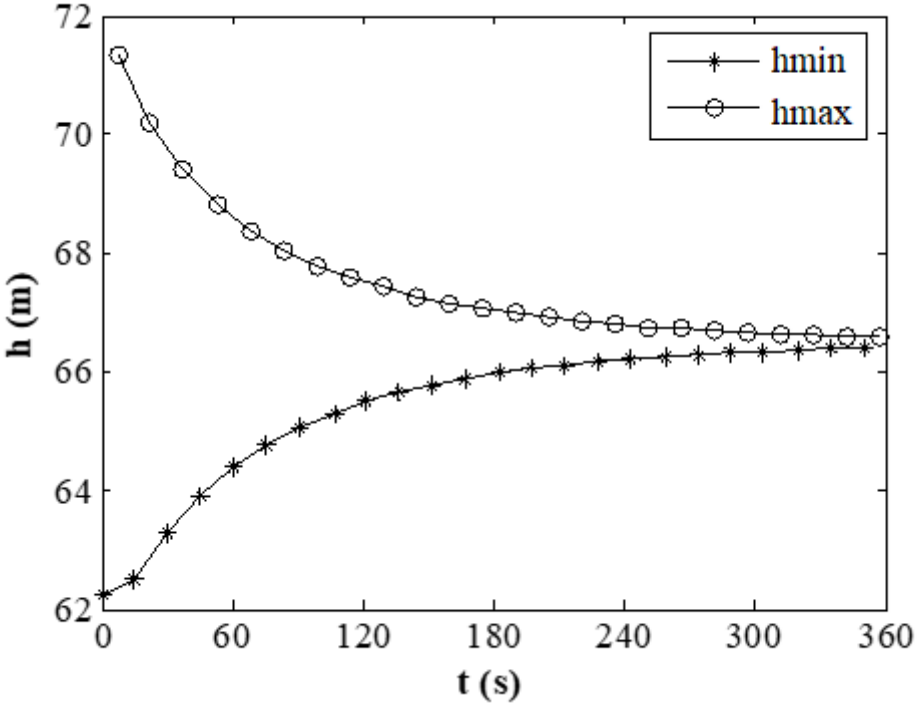

Figure 9

Variations of minimum and maximum peaks associated with head pressure in the surge tank

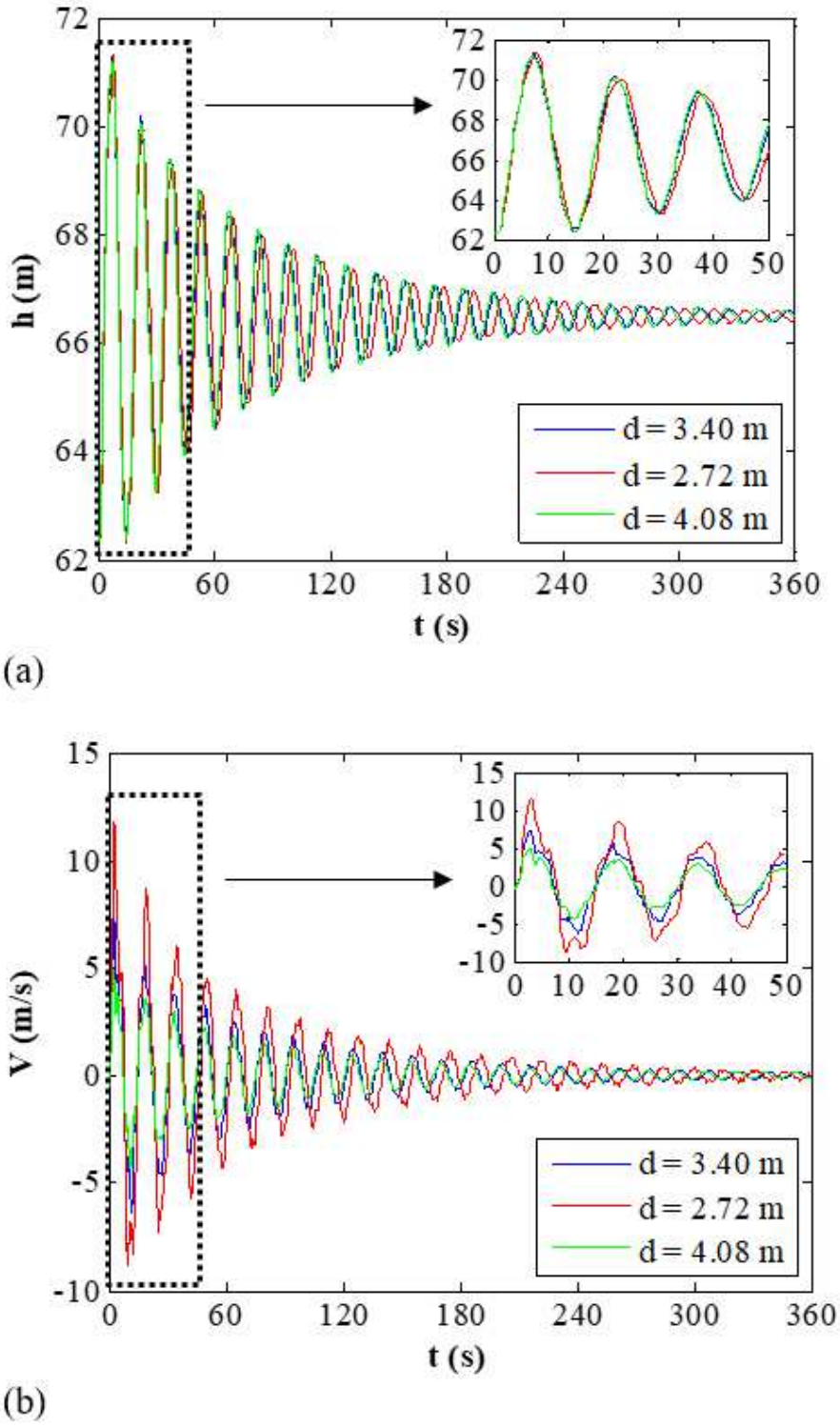

Figure 10

Variations of surge tank response versus inlet diameter: (a) head pressure, and (b) flow velocity

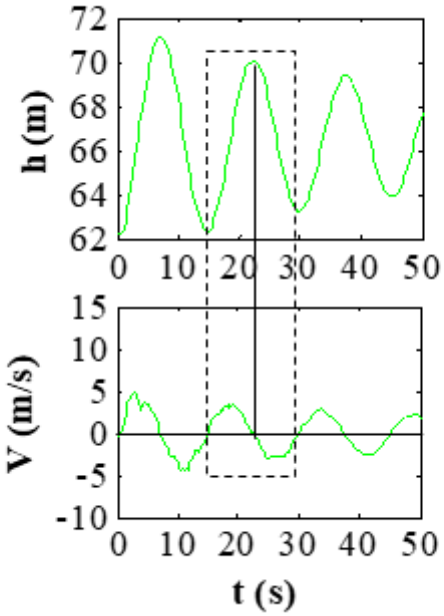

Figure 11

Response of the surge tank

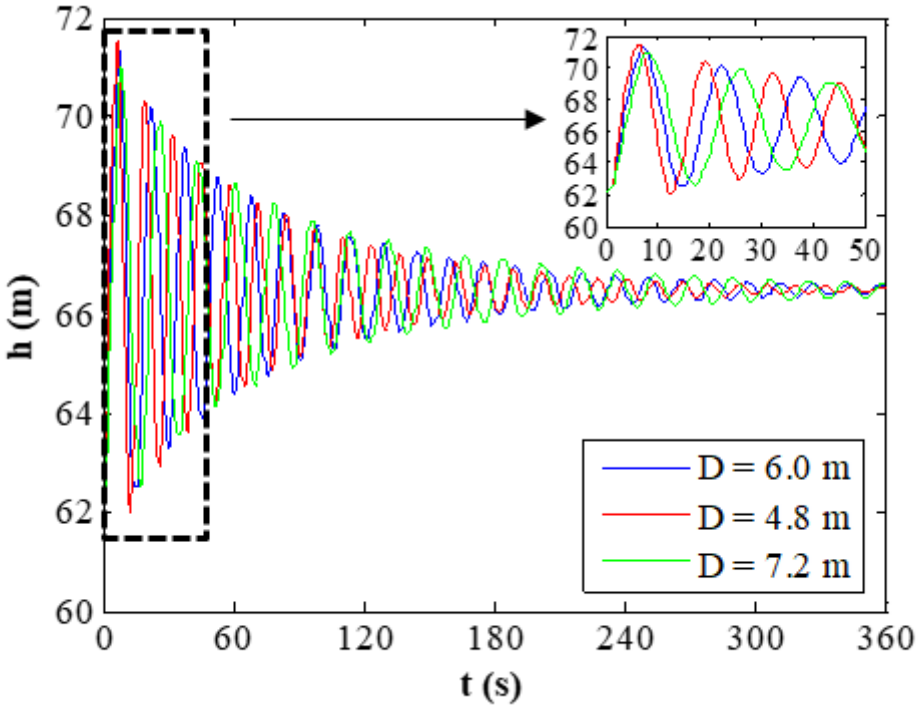

Figure 12

Variations of head pressure fluctuations for various values of surge tank diameter

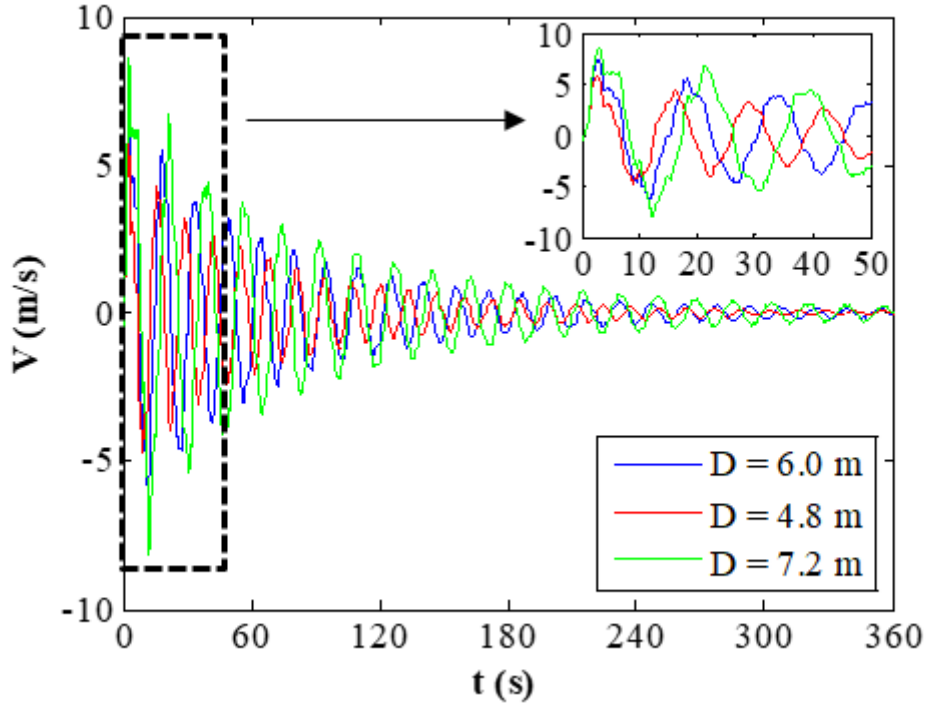

Figure 13

Variations of flow velocity fluctuations for various values of surge tank diameter

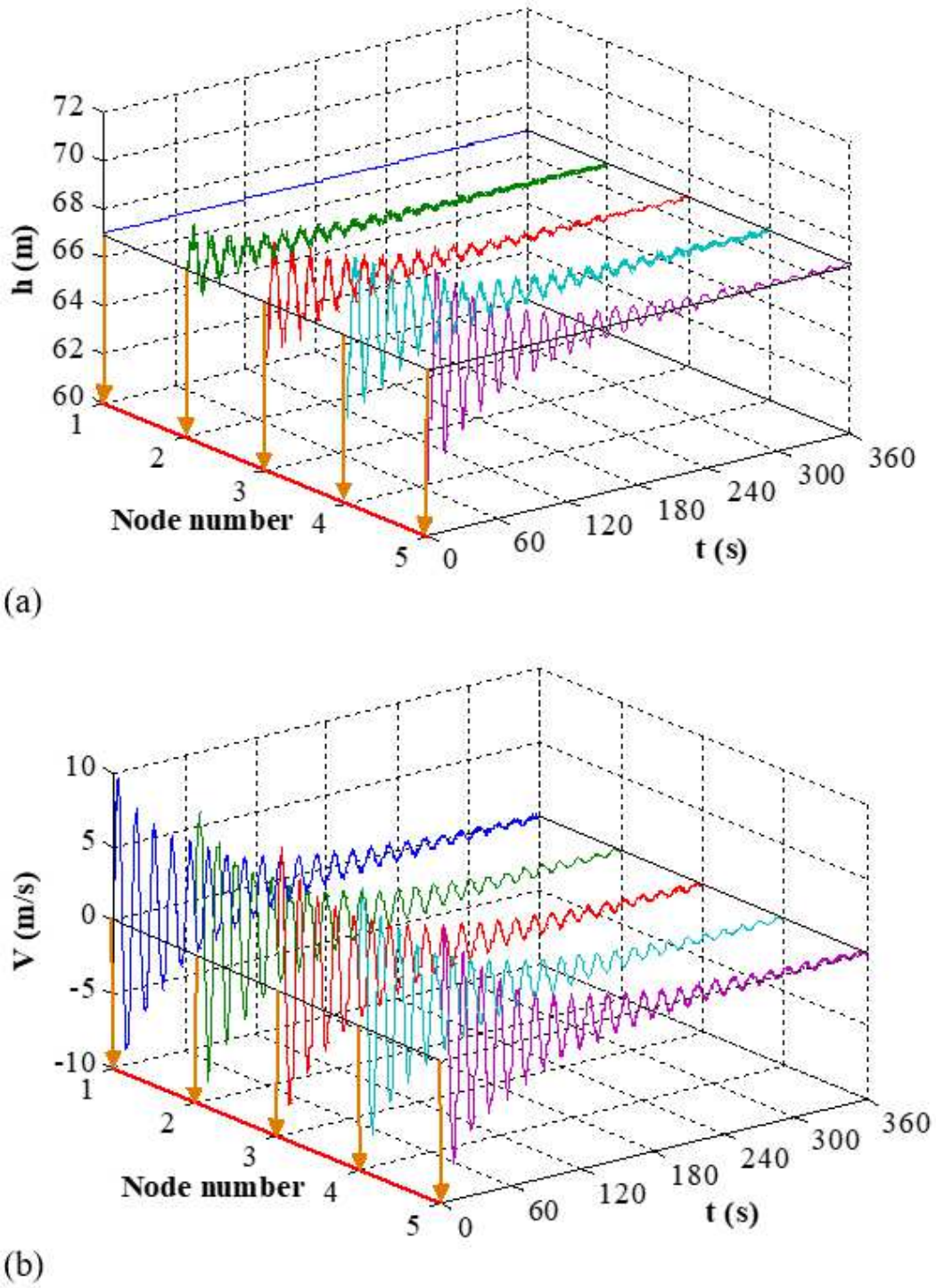

Figure 14

Variations of upstream pipeline of surge tank for nodes 1 to 5: (a) head pressure, and (b) flow velocity

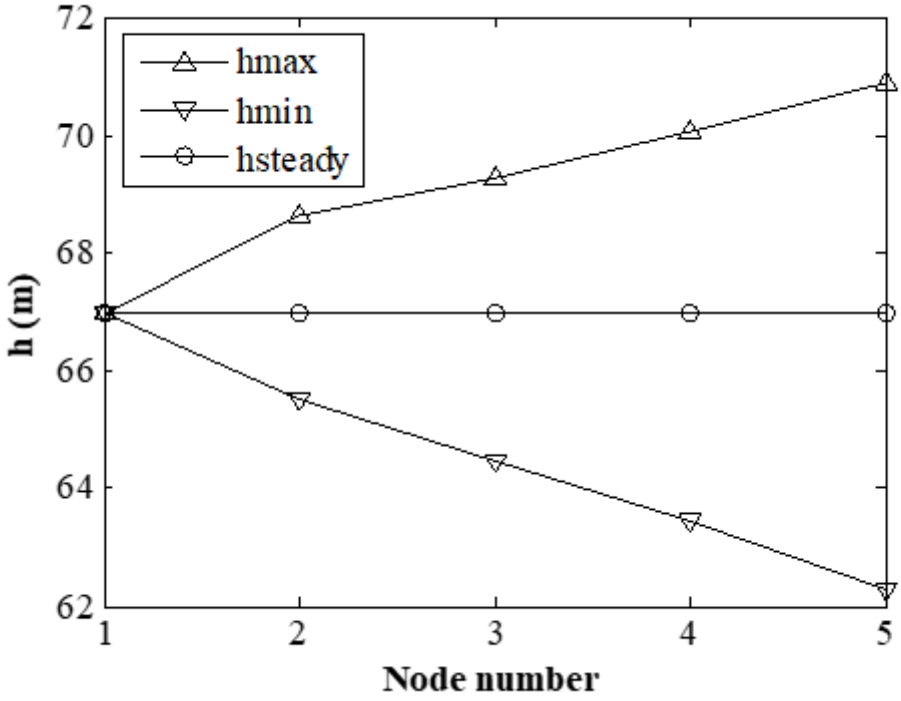

Figure 15

Minimum and minimum values of head pressure at nodes 1 to 5

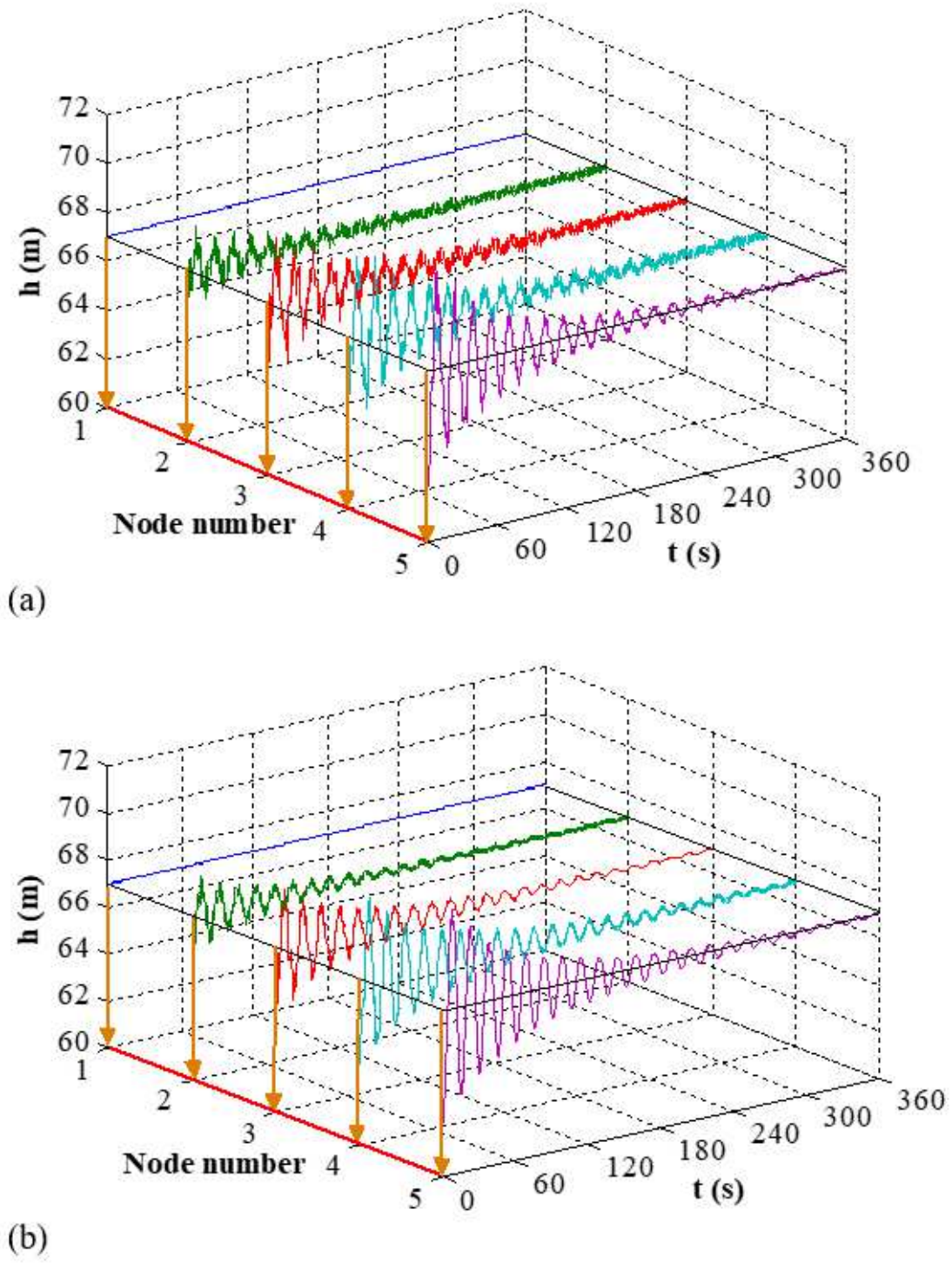

Figure 16

Variations of maximum difference in the head pressure for nodes 1 to 5 versus various values of surge tank inlet diameter (a) d=2.72 m, and (b) d=4.08 m

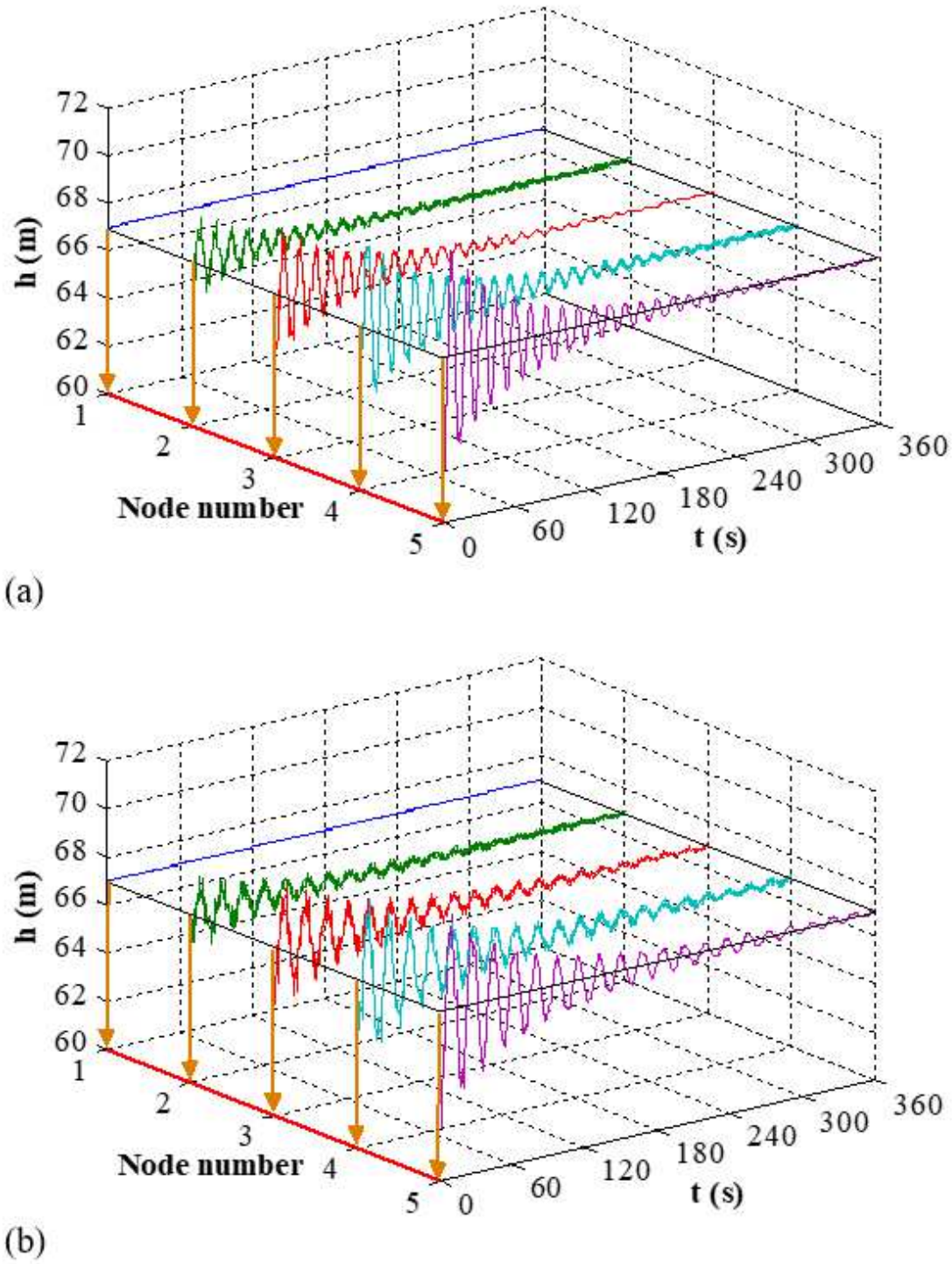

Figure 17

Fluctuations of head pressure at upstream of surge tank with different diameter: (a) D=4.8 m and (b) D=7.2 m

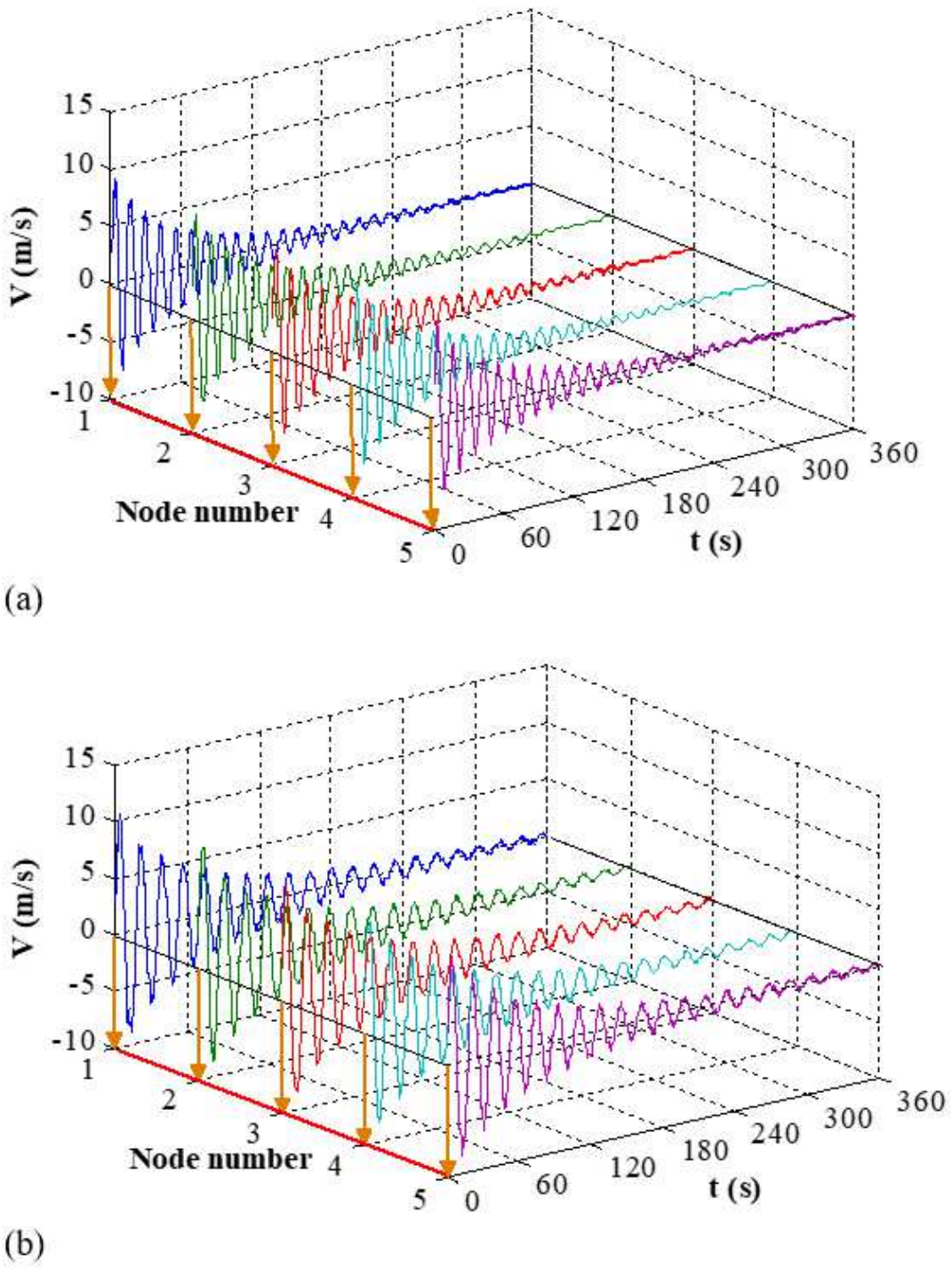

Figure 18

Maximum difference in the flow velocity at upstream of surge tank with different diameter: (a) D=4.8 m and (b) D=7.2 m